Circuit Quantum Electrodynamics: A Scalable, Modular Quantum Information Processing Architecture

Matthew Beck

Physics 801

Spring 2013

1 Introduction

Since its advent less than a decade ago, *circuit* quantum electrodynamics (cQED) has been the focus of intense research. Borrowing a page from cavity quantum electrodynamics (CQED) developed in the quantum optics community, cQED aims to test, measure, and control the fundamental interactions between light and matter at the single photon level in which the lasers, optical cavities, and atoms of CQED have been replaced with superconducting microwave transmission lines, resonators and Josephson Junctions (JJ's)[1]. Presented here is a brief synopsis of the underlying theory and implementation of cQED cast in the light of a scalable quantum information processing (QIP) architecture.

2 Governing Dynamics

As previously mentioned, cQED aims to study the interactions between EM waves and matter at the single photon, single atom level. Such interactions can be described by the Jaynes-Cummings Hamiltonian [2]

$$H_{JC} = H_{res} + H_{Atom} + H_{int} = \hbar\omega_r(a^\dagger a + 1/2) + \frac{\hbar\omega_a\sigma_z}{2} + \hbar\gamma(a^\dagger\sigma_- + a\sigma_+) \quad (1)$$

Where it is assumed that the EM wave is confined within a cavity and the atom term is taken to be a Fermionic spin 1/2 two level system (TLS). The first term in H_{int} describes the relaxation of the TLS from $|e\rangle$ to $|g\rangle$ through the spontaneous emission of a photon into the cavity. The second term describes the absorption of a photon from the cavity to promote the TLS to $|e\rangle$. The rate at which both processes take place is γ.

Although H_{JC} can be solved exactly[3], there are two particular limiting cases that are of particular interest, namely the dispersive limit ($\omega_r - \omega_a = \Delta >> \gamma$) and the strong coupling limit ($\omega_r = \omega_a = \omega$).

In the dispersive limit, H_{int} can be treated perturbatively[4]. Working through the machinery of non-degenerate perturbation theory, one arrives at a second order energy correction to the atom / TLS energy of the form $\hbar\gamma^2(2n+1)/\Delta$. This can be treated as an effective shift in resonant frequency yielding

$$H_{Atom} = \frac{\hbar\sigma_z}{2}(\omega_a + \gamma^2(2n+1)/\Delta) \quad (2)$$

Alternatively, one can solve for the dynamics in the interaction picture to obtain a second order shift energy shift now treating the resonator as the system being perturbed.

$$H_{res} = \hbar(\omega_r + \frac{\gamma^2\sigma_z}{\Delta})(a^\dagger a + 1/2) \tag{3}$$

What one sees is that in the dispersive limit where the two systems are far detuned and decoupled, the cavity state can be used as a direct probe of the state of the TLS or vice versa. This type of indirect measurement where

$$[H_{atom}, H_{total}] = [H_{res}, H_{total}] = 0 \tag{4}$$

is a concrete example of what is called quantum non-demolition (QND)[5], where the measurement and its necessary back action projects the measured system into a state that is correlated with the measurement outcome. This allows for the same measurement to be repeated numerous times yielding the same result in order to build up statistics.

In the strong coupling regime, H_{JC} is diagonal in the $|\psi\rangle = 1/\sqrt{2}(|n, e\rangle \pm |n+1, g\rangle)$ basis [4]. The difference in energy between these two states in proportional to $\sqrt{n}$, (where $n = a^\dagger a$, the cavity excitation occupation number) which in effect creates an strongly anharmonic ladder of energy eigenstates. By systematically "climbing" the energy ladder through coherent excitations between the resonator and TLS, one can prepare an arbitrary Fock number state[6] that can be effectively mapped into the computational basis of $|0\rangle, |1\rangle$ and utilized for QIP.

3 Implementation

The physical realization of such an interaction scheme is done through the use of superconducting (SC) microwave resonators and qubits. The qubits are derived from novel geometries involving one or multiple JJ's[7] and come in three flavors: Charge, flux and phase. In terms of the resonators, many different geometries exist including microstrip, stripline, and coplanar waveguide (CPW) geometries[8]. Any of these particular elements can be fabricated in and integrated design using standard lithographic techniques. While in the following sections all three flavors of qubits will be sampled, only CPW resonator geometry will be focused on.

3.1 Charge Qubit

The charge qubit, also known as a cooper pair box (CPB), connects a superconducting island to a grounded reservoir via a JJ[9]. By applying a capacitively coupled gate voltage, one can induce cooper pairs to tunnel across the junction and effectively change the number of cooper pairs on the island. This coherent interaction between the island and reservoir, mediated by the cooper pair tunneling, quantizes the charge states on the island. The dynamics describing the CPB

is the sum of two terms; the electrostatic charge energy stored on the island and the JJ tunneling [10].

$$H_{CPB} = H_{charge} + H_{JJ} = 4E_c(\tilde{N} - n_g)^2 \left|n\right\rangle \left\langle n\right| - \frac{E_j}{2}(\left|n\right\rangle \left\langle n+1\right| + \left|n+1\right\rangle \left\langle n\right|) \quad (5)$$

Where $n_g = \frac{C_g V_g}{2e}$, the number of cooper pairs on the gate capacitor. Without the tunneling energy, the CPB becomes degenerate to first order for successive charge states at a bias point of $n_g = n + 1/2$. The tunneling energy lifts this degeneracy but the average charge number $\langle \tilde{N} \rangle \rightarrow$ n/2, denoting charge frustration which can only be described as the symmetric/antisymmetric superpositions of successive charge states[4].

Restricting to the first 2 charge basis states ($\left|0\right\rangle, \left|1\right\rangle$) and to first order in n_g, H_{CPB} can be written as

$$H_{CPB} = \frac{1}{2}\begin{pmatrix} -E & -E_j \\ -E_j & E \end{pmatrix} = \frac{1}{2}\left(E\sigma_z - E_j\sigma_x\right) \quad (6)$$

Where $E = 4E_c(1 - 2n_g)$.

This new representation is the same as that of a spin 1/2 subject to a magnetic field with only x and z components. One can rotate through an angle $\phi = \arctan(\frac{-E_j}{E})$ to retrieve quantization in the $\hat{z}$ direction with a final hamiltonian of $H = \hbar\omega'\sigma_z$, where $\omega' = \sqrt{E^2 + E_j^2}$.

3.2 Flux Qubit

The flux qubit consists of a superconducting loop interrupted by one or more JJ's [11]. The Hamiltonian is [12]

$$H_{Flux} = \frac{q^2}{2C_{JJ}} + \frac{\phi^2}{2L} + E_{JJ}\cos(\frac{1}{\Phi_0}(\phi - \phi_{ext})) \quad (7)$$

Where Φ_0 is the flux quantum. A consequence of superconductivity is flux quantization through inductive loops[13] allowing one to rewrite $\phi \rightarrow \tilde{N}\Phi_0$. This now looks semi similar to the Hamilotonian for the CPB. Flux biasing this circuit at $\phi_{ext} = \Phi_0/2$ (flux is the conjugate to charge) creates flux frustration in which the solution to (7) is a linear superposition of counterpropogating currents in the SC loop.

Indeed, (7) can be rewritten in a spin 1/2, TLS format[12] in which, for sake of brevity, is only presented and not derived.

$$H_{flux} = E'(\sigma_z + \alpha\sigma_x) \tag{8a}$$
$$\alpha \propto E_L/E_{split} \tag{8b}$$
$$E' = E_{split}/2 \tag{8c}$$
$$E_{split} = \eta\sqrt{E_b E_c} Exp[-\zeta\sqrt{E_b/E_c}] \tag{8d}$$
$$E_b = E_{JJ}3\lambda^2/2 \tag{8e}$$
$$\lambda = L_{JJ}/L_{loop} - 1 \tag{8f}$$

Where $E_{c,L}$ is the energy stored in the effective capacitance/inductance of the junction and η, ζ are constants.

3.3 Phase Qubit

The current and voltage across a JJ are related to the phase across the boundary in the following ways [14].

$$I_{JJ} = I_0 \sin(\delta) \tag{9a}$$
$$V_{JJ} = \frac{\Phi_0}{2\pi}\frac{d\delta}{dt} \tag{9b}$$
$$\delta = \phi_1 - \phi_2 \tag{9c}$$

Differentiating (9a) and combining with (9b) and $V = LdI/dt$ one arrives at $L = \Phi_0/(2\pi I_0 \cos(\delta))$. Solving for the energy

$$E = \int Pdt = \int I_{JJ}V_{JJ}dt = \frac{I_0\Phi_0}{2\pi}\sin(\delta)\frac{d\delta}{dt}dt = -\frac{I_0\Phi_0}{2\pi}\cos(\delta) \tag{10}$$

If the same calculation is repeated only with a current bias across the junction, the potential energy takes the form $U = -\rho(\delta + \cos(\delta))$ which is commonly called the "tilted washboard" potential. The local minima of the potential can be approximated as a quadratic / harmonic oscillator-esque type potential [15] that can and does support anharmonically spaced bound states. The $|0\rangle, |1\rangle$ states, otherwise known as the current and voltage states can be put into a linear superposition by applying a microwave drive pulse [16] tapped into the circuit at the resonant transition frequency. A measurement of the qubit state is done by applying a large microwave pulse to the qubit for which the $|1\rangle$ state will tunnel out of the local potential creating quasiparticles and a measurable voltage across the junction [15].

3.4 CPW Resonator

The CPW resonator is a two dimensional analog of a coaxial cable . It consists of a center conducting strip surrounded by a ground plane on both sides deposited on

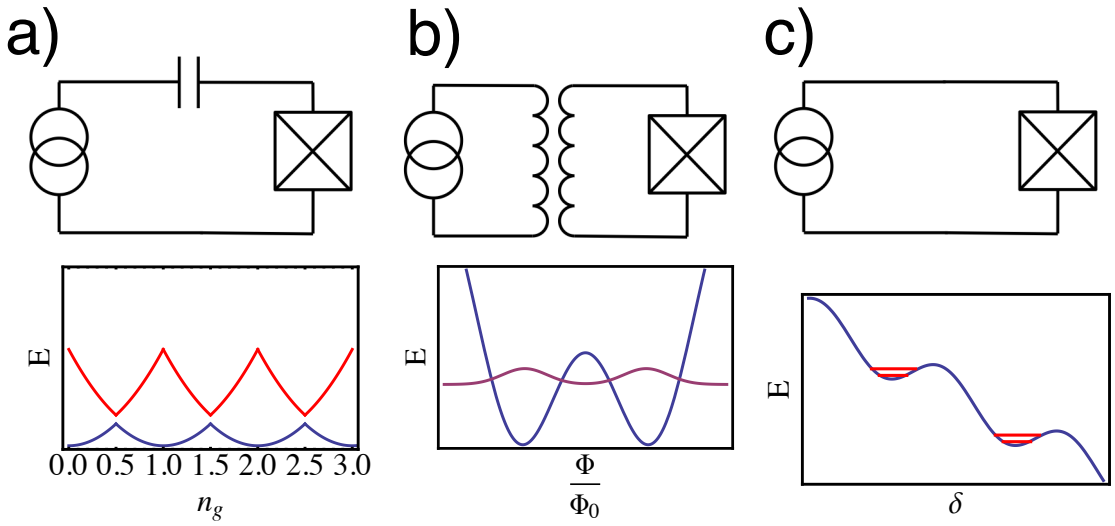

Figure 1: The three SC qubits. **(a)** Charge qubit circuit schematic where the boxed cross is the JJ. **(b)** Circuit schematic for an inductively coupled flux qubit. **(c)** Circuit schematics for the phase qubit. The bottom row shows the potential landscape with representative bound state wave functions for the three qubits.

top of a dielectric. CPW's have gained preference amongst researchers in cQED through their strongly geometry dependent impedance / inductance along with ease of fabrication, and relatively high quality factors (10^5) [17].

There are two general geometries in which CPW's are used. In both geometries, the input of the center conducting strip is capacitively / gap coupled to a microwave feed line that induces the excitation. The difference lies in whether or not the output of the center line is capacitively coupled out to a transmission line or grounded. For the first coupled output, solving for the boundary conditions yields field antinodes at the ends of the conductor yielding $n\lambda/2$ resonant modes in the resonator. Should the output end be grounded, one finds that there must be a antinode / node at the input / output yielding $(2n+1)\lambda/4$ resonant modes [18], which cannot be formed in traditional high finesse Fabry-Perot cavities [19].

3.5 Coupling The Cavity and Qubit

In the CPW resonator geometry, the interaction term, H_{int}, can be realized by placing the qubit at the antinode of the resonator (see Fig.2b) [4]. Near resonance, cavities can be approximated as a lumped tank LC oscillator [20]. In this near resonance regime, the coupling strength, γ, between the CPW and qubit can be approximated as [21]

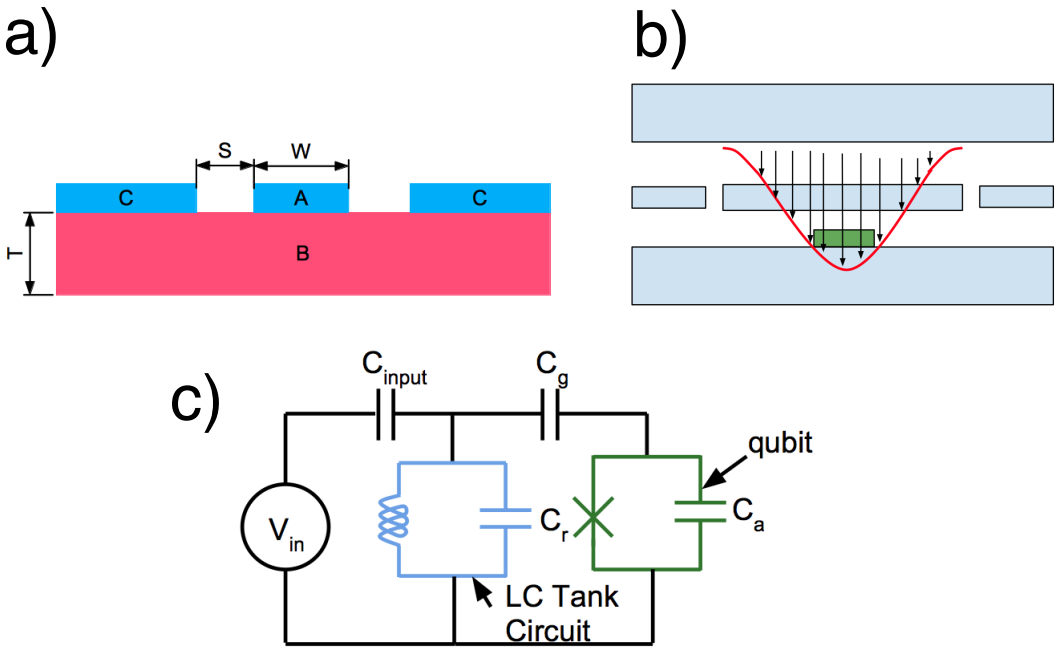

Figure 2: **(a)**Cross section view of the CPW geometry. A is the center conducting strip. B is the dielectric and C are the ground planes. The ratio k = s/w is the defining geometric variable that defines the impedance and inductance [Citation]. **(b)** Aerial view of a qubit (shown in green) placed at the antinode of the CPW resonator. Blue are the conducting wires / ground plane while white is the substrate. **(c)** Equivalent lumped element tank LC circuit for near resonance performance of the CPW and qubit.

$$\gamma = \frac{C_{gate}}{2}\sqrt{\frac{\omega_r \omega_a}{C_a C_r}} \tag{11}$$

Where ω_a, ω_r are the resonant frequencies of the qubit and resonator, respectively. The C_a term arises by treating the Josephson element as a purely inductive element in parallel with a capacitor, C_a. The gate capacitance is the capacitance between the center conducting wire and the qubit and C_r is the capacitance for the equivalent LC oscillator circuit for the CPW.

4 Concluding Remarks

cQED shows promise as a QIP architecture. Its integrated modularity and standard fabrication techniques allows one to imagine scaling from one qubit - resonator pair to a large IC consisting of thousand to millions of qubit-resonator pairs. Re-

cent work done by the Martinis group at UCSB [22] has utilized IC consisting of over 100 SC flux qubits to solve for the ground states of an Ising spin-glass, a classical NP-hard problem [23]. In addition, novel manipulation and trapping of photons has been demonstrated [24].

Scalability in qubit density / IC size isn't the only future path foreseen for cQED. Current work at the University of Wisconsin - Madison and elsewhere [25] is attempting to bridge the gap between cQED and CQED by creating a coherent neutral atom - SC resonator - SC qubit interface in which the long coherence times of neutral atom Rydburg states ($\sim$ 1s) can be coupled with the GHz processing speed of the superconducting circuits.

In all, cQED, possessing a tool box of qubits and resonators, is a maturing science with the capability to measure fundamental light - matter interactions at the single photon, single atom limit. It is the ability to reach this limit and the strong coupling regime that ultimately make cQED a strong candidate for the realization of a full scale quantum computer.

5 References

[1] Wallraff, A., et al. Circuit Quantum Electrodynamics: Coherent Coupling of a Single Photon to a Cooper Pair Box, *Nature (London)* 431, 162-167 (2004)

[2] Jaynes, E. T.,Cummings, F. W. Comparison of quantum and semiclassical radiation theories with application to the beam maser, *Proceedings of the IEEE* 51, 89109 (1963)

[3] Agarwal, G. *Quantum Optics*, Cambridge University Press, (2013)

[4] Schuster, David. *Circuit Quantum Electrodynamics*, PhD Thesis, Yale, (2007) http://www.eng.yale.edu/rslab/papers/

[5] Benson, O., Lenneberger, F. *Semiconductor Quantum Bits*, Pan Stanford, (2008)

[6] Hofheinz, M. et al. Generation of Fock states in a superconducting quantum circuit, *Nature* 454, 310-314 (2008)

[7] Martinis, J. Superconducting Qubits and the Physics of Josephson Junctions, *Les Houches Session LXXIX (2003): Quantum Entanglement and Information Processing*, 487-520 (2004)

[8]Golio, M. *The RF and Microwave Handbook*, CRC, (2001)

[9] Cottet, A. *Implementation of a quantum bit in a superconducting circuit*, PhD Thesis, University of Paris, (2002) http://www.phys.ens.fr/∼cottet/

[10] Bouchiat, V. *Quantum Fluctuations of the charge in single electron and single Cooper pair devices*, PhD Thesis, University of Paris, (1997)

[11] Clark, J. et al. Quiet readout of superconducting flux states, *Phys. Scr*, (2002)

[12] Devoret, M. H. et al. Superconducting Qubits: A Short Review, arXive: cond-mat/0411174 (2004)

[13] Doll, R., Nabauer, M. Experimental proof of magnetic flux quantization in a superconducting ring, *PRL* Vol. 7,No.2, (1961)

[14] Van Duzer, T. *Principles of Superconductive Devices and Circuits, 2e*, Prentice Hall, (1999)

[15] Mitra, K. et al Qauntum behavior of the dc SQUID phase qubit, *Phys. Rev. B* 77, 214512 (2008)

[16] Neeley, M. et al Process tomography of quantum memory in a Josephson-phase qubit coupled to a two-level state, *Nature Physics* Vol. 4 (2008)

[17] Goppl, M. et al. Coplanar waveguide resonators for circuit quantum electrodynamics, *J. Appl. Phys.* 104, 113904 (2008)

[18] Wu, X. et al. Quality factors of coplanar wave guide resonators, *Microwave Conference*, (1999)

[19] Toal, V., *Introduction to Holography*, CRC Press, (2012)

[20] Pozar, D., *Microwave Engineering, 3e*, John Wiley, (2005)

[21] Girvin, S. M., et al *Phys. Scr.* (2009)

[22] Boixo, S., Qunatum annealing with more than one hundred qubits, arXiv:1304.4595 (2013)

[23]Barahona, F., On the computational complexity of Ising spin glass models, *J. Phys. A: Math. Gen* 15 3241 (1982)

[24] Sete, E., Catch-Disperse-Release Readout for Superconducting Qubits, arXiv:1302.7020(2013)

[25] Bernon, S., Manipulation and coherence of ultra-cold atoms on a superconducting atom chip, arXiv:1302.6610 (2013)